Turkish Journal of Electrical Engineering & Computer Sciences

http://journals.tubitak.gov.tr/elektrik/

Research Article

Turk J Elec Eng & Comp Sci
(2020) 28: 2316 – 2330

doi:10.3906/elk-2002-99

On a yearly basis prediction of soil water content utilizing sar data: a machine learning and feature selection approach

Emrullah ACAR[1,*], **Mehmet Siraç ÖZERDEM**[2]

[1]Department of Electrical and Electronics Engineering, Batman University, Batman, Turkey
[2]Department of Electrical and Electronics Engineering, Dicle University, Diyarbakır, Turkey

Received: 15.02.2020 • **Accepted/Published Online:** 05.04.2020 • **Final Version:** 29.07.2020

Abstract: Soil water content (SWC) performs an important role in many areas including agriculture, drought cases, usage of water resources, hydrology, crop diseases and aerology. However, the measurement of the SWC over large terrains with standard computational techniques is very hard. In order to overcome this situation, remote sensing tools are preferred, which can produce much more successful results in less time than standard calculation techniques. Among all remote sensing tools, synthetic aperture radar (SAR) has a significant impact on determining SWC over large terrains. The main objective of this study is to predict SWC on a yearly basis over the vegetation-covered terrains with the aid of different machine learning techniques and SAR based Radarsat-2 data, which obtained in 2015 and 2016 years.The proposed system consists of several stages, respectively. In the feature extraction stage, the backscatter coefficients of different polarizations and the parameters obtained from different models of decomposition (Freeman-Durden and H/A/α) were combined and nine polarimetric features were formed for each sample point. In the next stage, support vector regression (SVR), generalized regression neural network (GRNN) and adaptive neuro-fuzzy inference system (ANFIS) were employed for the prediction of SWC. In the last stage, a machine learning based feature selection was implemented to the obtained feature vectors for determining optimal feature sets. Finally, a feature set with 6 parameters was determined as most optimal feature set over the SWC prediction and a slightly better performance was observed thanks to this feature set compared to the other results.

Key words: Synthetic aperture radar, support vector regression, generalized regression neural network, adaptive neuro-fuzzy inference system, feature selection, soil water content

1. Introduction

Soil water content (SWC) plays substantial role in many areas such as minimizing the destructive effects of drought cases, avoiding saltiness caused by over watering, keeping from the harm agricultural areas and utilization of the irrigation system efficiently. With the rapid and reliable prediction of the SWC level, the damages on these areas can be diminished. The measurement of SWC over wide agricultural fields by standard computational techniques, which consist of direct (gravimetric measurement) and indirect (time domain reflectometry, neutron meter, tensiometer, conductive and thermal sensors, frequency-effect reflectance meter) methods is quite expensive and difficult. Whereas, current information obtained from remote sensing tools reach their target in a shorter time with less cost comparing to standard computational techniques [1]. Easy update of remote sensing technology provides a great advantage over other standard methods. Moreover, the ability to work even in difficult geographical regions can be listed as other important advantage of this technology

*Correspondence: acar_emrullah@hotmail.com

[2]. Among different types of remote sensing tools, SAR sensor has a great potential in SWC prediction over large areas [3]. Thus, many remarkable studies that are related to SAR data, have been investigated to calculate SWC parameters for 30 years. A SAR system can own diverse levels of polarization complexity which includes single (hh or vh or hv or vv), dual (vv+vh, hh+hv or hh+vv) and polarimetric (hh, hv, vh and vh). Among those polarizations, the polarimetric SAR can provide more detailed data by multiple polarizations and penetrate the bare and vegetated surfaces. It can also generate appropriate high resolution images for soil monitoring and agricultural mapping [4]. Prediction of SWC on vegetation-covered agricultural areas is very difficult since it requires complex processing. The reason for this situation is that the backscattering originating from the vegetation cover affects the scattering from the target point. Two main distinct scattering techniques have been used in the literature to diminish the effect of vegetation scattering from the canopies and form feature vector from SAR data. These are polarimetric decomposition models and multiple configuration SAR techniques [5]. Among these techniques; Touzi and Yamaguchi, Freeman-Durden, Krogager and H/A/α, are the most popular for feature extraction stage and several literature studies have been made with the aid of them [6–9]. In our study, H/A/α; Freeman-Durden and standard intensity/phase techniques were employed for feature extraction. Because these techniques help to diminish the backscattering caused by canopies on the grounds, where the vegetation is dominant [10].

Following the stage of feature extraction, different inversion techniques have been improved for prediction of the soil surface parameters in the literature. These inversion techniques are based on the empirical/semi-empirical [11], theoretical [12] and machine learning approaches[13–18]. Among these approaches, machine learning is the most effective inversion technique since the other techniques have limited application areas as well as depend on area-specific surface parameters and experimental equations [13, 14]. Machine learning methods include partial least squares regression, support vector machines, extreme learning machine, the cubist regression, Bayes and neural networks, are the mostly employed inversion techniques for SWC prediction [19–26]. In our study, for prediction of SWC on a yearly basis, support vector regression (SVR), adaptive neuro-fuzzy inference system (ANFIS) and generalized regression neural network (GRNN) are proposed because of their fast learning ability and good predictive properties.

In the last phase, the most effective polarimetric features have been selected successfully with the aid of feature selection methods. The duty of the feature selection is to obtain a subset of the most appropriate features for a similar or better prediction instead of using all the features. Different procedures have been asserted for feature selection, including the sequential forward selection [27–29], ReliefF and sequential backward selection [30]. However, there are still several problems in the above methods such as the inadequacy of relations between the features, the complexity of high computation, monotonicity of objective function [31]. Therefore, a new approach using extreme learning based feature selection (ELM-FS) is preferred in this study since it has fast learning speed and good generalization performance comparing to the other methods [32].

The main objective of this research is to predict SWC on a yearly basis approach over the vegetation-covered terrains with the aid of polarimetric SAR features. Moreover, there are 2 main contribution of this paper. One of them is that feature vector for each sample point was obtained by a novel approach as combining polarimetric features acquired from standard intensity/phase technique and different polarimetric decomposition models (Freeman-Durden and H/A/α). Another one is that the soil water content (SWC) values were predicted in a new manner on a yearly basis with the aid of different machine learning based prediction and feature selection techniques.

2. Materials and methods

2.1. Working area

The working area includes 2 distinct terrains covering an average of 2×3 km^2 and 4×4 km^2 of frame within Dicle University campus in the province of Diyarbakır, Turkey (40°04'-40°26'E, 37°46'-38°04' N). The average area slope is 3.05% and the average height is 650 m. The yearly average maximum temperature is 34.5 °C and 8.2 °C in the summer and winter, respectively. Moreover, the yearly average temperature is 23.8 °C and the rainfall is 496.0 mm. The working area is covered by cultivated fields containing large quantities of wheat and barley throughout the Radarsat-2 transition periods. The position of the working area is presented in Figure 1.

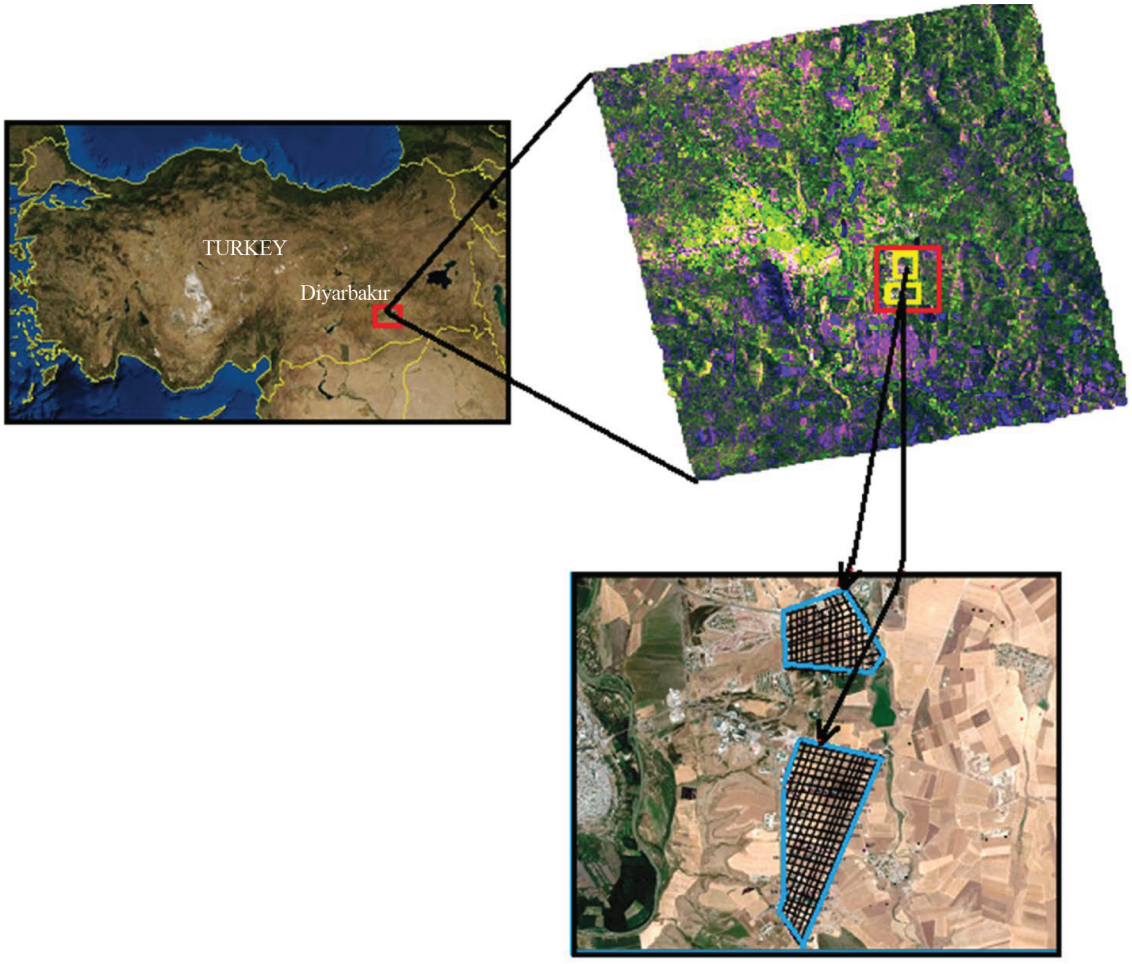

Figure 1. The geographic position of the working area. The red square shows the pilot areas.

2.2. Data collection

In this work, 4 fully polarimetric Radarsat-2 images were obtained in different times of cultivation period. These Radarsat-2 products are in the single look complex (SLC) data format that hold amplitude, resolution and phase information of Radarsat-2 data and have 5.83 m spatial resolution and 30×30 km^2 coverage. The general properties of the obtained SAR data are indicated in Table 1.

Table 1. The general properties of the obtained Radarsat-2 data.

Dates	Time	Beam	Pass
27/02/2015	03:17:42	FQ24	Descending
08/04/2015	15:07:11	FQ4	Ascending
10/06/2015	03:10:31	FQ29	Descending
03/03/2016	03:25:47	FQ13	Descending

After Radarsat-2 data acquisition, working area was divided into 100 × 100 meter grids and ground soil samples were taken 3–5 cm deep from the surface of these grids. An average of 250–300 soil samples was collected during the each satellite transition over the experimental area. These samples were then filled into 100 cm^3 metallic containers and their locations were recorded with the aid of the GPS tools. SWC values of obtained local soil samples were then calculated by gravimetric technique in the Science and Application Research Center of Dicle University and presented in Table 2.

Table 2. Local measurement values of SWC (%) for each period.

Evaluation period	Pilot area	# of measurement points	Min SWC	Max SWC	Mean SWC	SD SWC
27/02/2015	Sparsely vegetated	335	18. 7	43. 6	29. 7	4.7
08/04/2015	Densely vegetated	285	20. 2	41. 3	30. 3	3.9
10/06/2015	Bare	272	0.8	44.7	7.4	7.0
03/03/2016	Moderately vegetated	157	25.3	43.2	34.4	2.8

2.3. Calibration-filtering and geocoding of Radarsat-2 data

The calibration-filtering and geocoding step was fulfilled in the following stages. First, Radarsat-2 images were read using the Sentinel-1 toolbox (S1TBX) and then calibrated for radiometric correction of these images. For diminishing the amount of the blurring and speckle noise on the Radarsat-2 data, a single product refined Lee filter was implemented. For terrain correction, SAR geometric distortions were corrected by employing a SRTM-3 digital elevation model and the filtered data was geocoded [33]. After that, universal transverse mercator (UTM) (WGS84) was preferred as output map projection. Lastly, the positions of the ground samples were then converted to .shp file format and imported to the Radarsat-2 images. The resulted images belonging to 4 different dates were indicated in the Figure 2 .

2.4. Producing Radarsat-2 data features

In this phase, for extracting feature vectors from the Radarsat-2 images, each pixel which corresponding to the GPS value of soil samples was symbolized by a cell or pattern (2 × 2 pixels). The backscattering coefficient of each pattern was then computed by mean of the coefficients in the cell. After that, the standard intensity/phase polarimetric features were obtained to generate feature vectors from the Radarsat-2 images. This step was followed by the polarimetric decomposition techniques (Freeman-Durden and H/A/α) and 5 more polarimetric features (volumetric, surface and double scattering with entropy and anisotropy) were calculated. The techniques used in the study for the feature extraction stage are described in detail by [34].

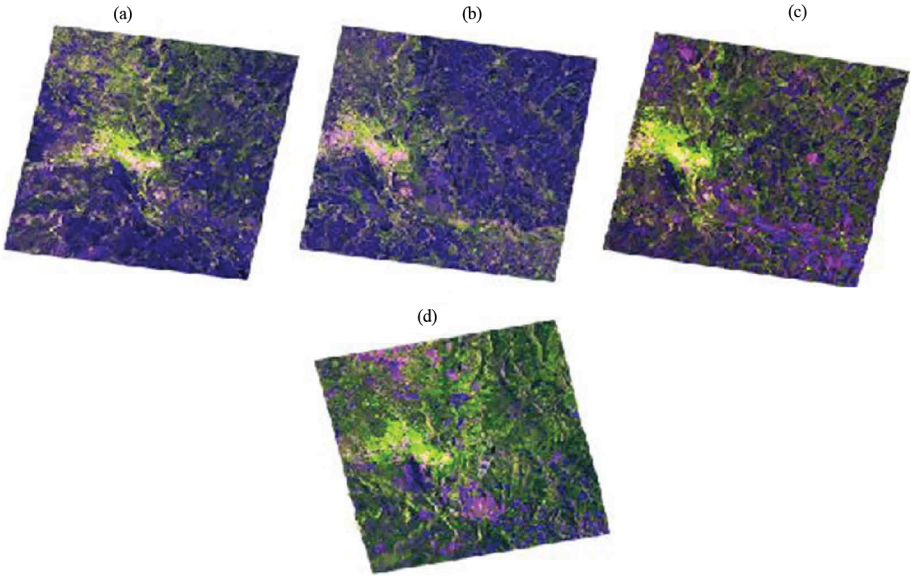

Figure 2. Calibrated-filtered and geocoded Radarsat-2 data which covers the Diyarbakır Province with different transitions: (a) Descending-27/02/2015; (b) Descending-10/06/2015, (c) Descending-03/03/2016 and (d) Ascendic-08/04/2015.

2.5. The standard phase and intensity polarimetric features

SAR is a type of radar that transmits electromagnetic wave to the target with vertical and horizontal polarization and measures the phase, polarization and intensity of backscattered waves from target. The polarimetric SAR system, which is another type of SAR, consists of 4 channels (σ_{hh}, σ_{hv}, σ_{vh} and σ_{vv}), in which information between the outgoing and back-scattered waves can be used to obtain information about the target object [35](Sakshaug et al., 2013). The main data format used to describe the backscattering is described in Equation 1). The elements in this matrix shows the distributions of polarization from horizontal to horizontal (hh), from vertical to horizontal (vh), from horizontal to vertical (hv), and from vertical to vertical (vv).

$$\begin{vmatrix} \sigma_{hh} & \sigma_{hv} \\ \sigma_{vh} & \sigma_{vv} \end{vmatrix} \tag{1}$$

2.6. Freeman-Durden polarimetric decomposition model

This model is based on 3 distinct scattering mechanisms with volume, double and surface scattering. In this model, the components are expressed in a physical interpretation and it is a very important model since it does not need for any ground measurements [36]. The volume scattering is modeled as reflection from the horizontally very thin, randomly oriented, cylinder-shaped dipole (scatterer) cloud. Besides this, the model required for the double bounce mechanism is based on the reflection from 2-plane corner reflectors. In this case, the 2 reflector surfaces can consist of different dielectric materials. For example, a trunk of tree and the soil surface can be used as 2-plane corner reflectors. Finally, surface scattering mechanism refers to scattering from a rough surface [37].

2.7. H/A/α decomposition model

Some of the polarimetric decomposition models are based on the eigenvector and eigenvalue separation of the coherency T3 or covariance C3 matrix. The H/A/α decomposition is one of these models and based on the eigenvector and eigenvalue analysis of the T3 coherent matrix, where the matrix T3 is expressed by Equation 2 [38].

$$\frac{1}{2}\begin{bmatrix} \left\langle \left|\sigma_{hh}+\sigma_{vv}\right|^2 \right\rangle & \left\langle (\sigma_{hh}+\sigma_{vv})\times(\sigma_{hh}-\sigma_{vv})^* \right\rangle & \langle 2\times\sigma_{hv}^*+(\sigma_{hh}+\sigma_{vv})\rangle \\ \left\langle (\sigma_{hh}-\sigma_{vv})\times(\sigma_{hh}+\sigma_{vv})^* \right\rangle & \left\langle \left|\sigma_{hh}-\sigma_{vv}\right|^2 \right\rangle & \langle 2\times\sigma_{hv}^*+(\sigma_{hh}-\sigma_{vv})\rangle \\ \left\langle 2\times\sigma_{hv}\left(\sigma_{hh}+\sigma_{vv}\right)^* \right\rangle & \left\langle 2\times\sigma_{hv}\left(\sigma_{hh}-\sigma_{vv}\right)^* \right\rangle & \left\langle 4\left|\sigma_{hv}\right|^2 \right\rangle \end{bmatrix} \tag{2}$$

2.8. Machine learning based regression models

In order to predict the SWC on a yearly basis over the bare and vegetated terrains, different machine based regression models: support vector machine (SVM), adaptive neuro-fuzzy inference system (ANFIS) and generalized regression neural network (GRNN) were used in this study. Among these models, GRNN is a powerful nonlinear machine learning technique proposed by Donald F. Specht and is included in the probabilistic neural network category. It needs only a part of the training set required for a back-propagation neural network. Thus, a probabilistic neural network can approach the basic function of the data even with only a few training examples [39, 40]. SVM is a supervised learning model that points to observe a hyper plane in the feature space and partition negative and positive samples with the lowest error rate [40]. SVM is generally employed in pattern recognition, classification and regression analysis. ANFIS is a hybrid model of Sugeno fuzzy logic inference systems and artificial neural networks. This model utilizes the neural network learning capability for the fuzzy inference system in order to calculate fuzzy rules more effectively and apply 3 fuzzy control steps (inference, fuzzification and defuzzification) [41].

2.9. ELM based feature selection (ELM-FS) method

The feature selection method is one of the significant issues in the areas of machine learning and it is generally used in the pattern detection and recognition applications [32]. The ELM, which has a high-speed training phase and good generalization capacity, is considered a fine approach for the feature selection method [42–44]. Although ELM is generally used as a machine learning method, it has been developed by [32] as a consistent, fast and independent feature selection algorithm with better accuracy [32]. In this method, biases and weights of the hidden layer are allocated indiscriminately, and the output layer's weights are computed with the aid of the Moore-Penrose approach [45, 46].The output of ELM, which has one single neuron, can be determined in Equation 3.

$$y_m = \sum_{i=1} \beta_{i,m} g(\sum_{j=1}^{k} w_{j,i} x_j + b_i) \tag{3}$$

Here, x_j and y_m indicates the input and m'th system output while k, l and m denotes neuron numbers of the input, hidden and output layers, respectively. Moreover, $w_{j,i}$ and $\beta_{i,m}$ indicate the assigned weights of the neurons which belong to the input and output layers, respectively. Additionally,b_i shows bias values which

implemented to the neurons in the hidden layer as well as $g(.)$ denotes the activation function applied for each neuron.

However, in ELM based feature selection approach, linear separable property of a function, $g(ax+b) = ag(x)+g(b)$, might be implemented to a transfer function g(.) in the hidden layer. Thus situated, Equation 3 can be rearranged as:

$$y_m = \sum_{i=1} \beta_{i,m} g(\sum_{j=1}^{k} w_{j,i} g(x_j) + g(b_i)). \tag{4}$$

At the end, the system equation turns into,

$$y_m = [\alpha(1,m), \alpha(2,m), ..., \alpha(j,m), ...\alpha(k,m)] \begin{pmatrix} x_1 & x_2 & . & . & .x_k \end{pmatrix}^T \tag{5}$$

Here, the obtained coefficient $\alpha(k,m)$ is the parameter that ranks the input elements of the system.The Equation 6 can be represented for a multi input and output system as

$$y_m = Ag([X^T]) + \epsilon \tag{6}$$

where, A, [X] and ϵ indicate coefficient matrix, input vectors and a scalar derived by β, respectively. The variation coefficient, $CV = \sigma/\mu$, has been then implemented to minimize the risk of obtained coefficients $\alpha(k,m)$ and computed for j'th input element of the system which denoted by $CV(x_j)$. Dividing the coefficients by $CV(x_j)$ revealed that if $CV(x_j)$ has low value, then the rank of x_j must be higher than compared to x_j which has high $CV(x_j)$ value. With the aid of this information, ranking of features (Fr) for ym in a feature selection stage can be represented as

$$Fr_{xj} = \left[\left| \frac{\alpha_{1,m}}{CV(x1)} \right|, \left| \frac{\alpha_{2,m}}{CV(x2)} \right|, ... \left| \frac{\alpha_{j,m}}{CV(xj)} \right|, ... \left| \frac{\alpha_{k,m}}{CV(xk)} \right| \right] \tag{7}$$

To summarize, feature selection procedure in the ELM-FS method depends on the number of elements used in the input and output of the system (k and m), the ranking coefficient $\alpha(k,m)$ and coefficient of variation $CV(x_k)$, respectively. In this work, we contemplate a multiple input for single output system, thus m is equal to 1 (m = 1). The number of elements at the input (x_j) is equal to the observation numbers in the obtained data sets $(j = 9)$ by considering the ELM training stage.

3. Results and discussion

In this section, prediction of SWC on a yearly basis was carried out on large terrains with the help of SAR datasets. Moreover, ELM-FS method was applied to determine optimal features of the proposed system. Two approaches have been considered in this system for SWC prediction. In the first approach, all obtained features were employed as inputs of machine learning model whereas in the second approach, only the selected feature sets were employed. The architecture of the recommended system was indicated in Figure 3.

3.1. SWC prediction with all features

In this stage, the datasets, which belong to 2015, and 2016 years were constituted from Radarsat-2 data. The feature vector for each pattern was obtained using standard intensity and phase as well as polarimetric

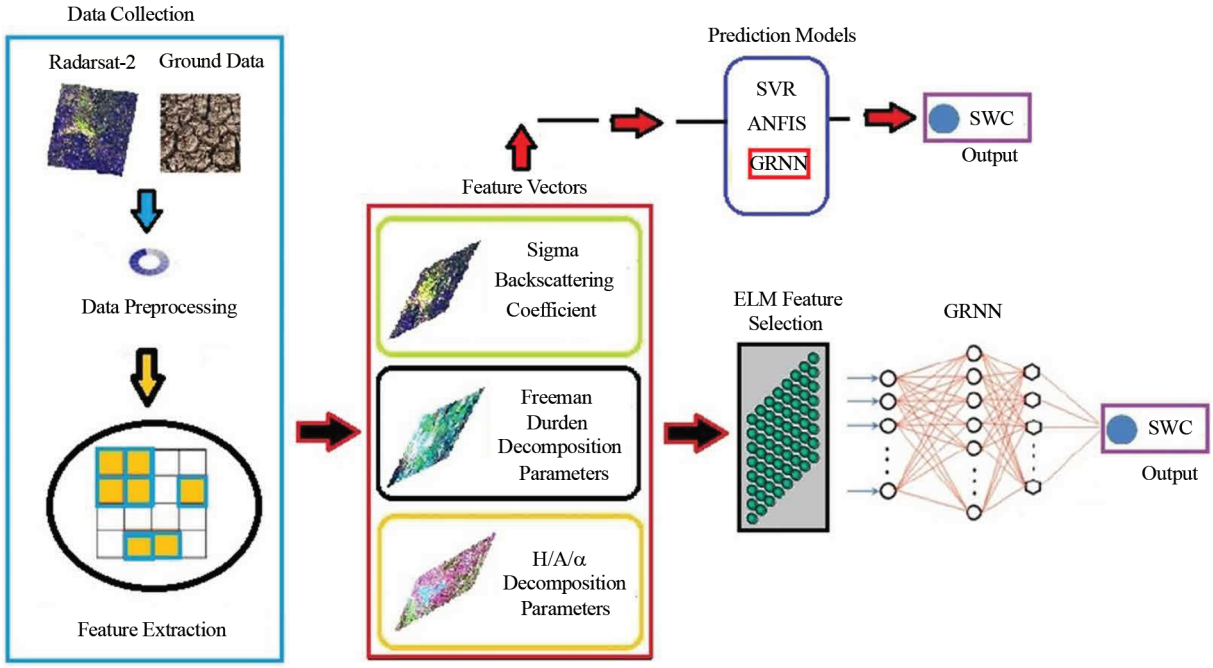

Figure 3. The architecture of the recommended system.

decomposition techniques. Then, totally 9 features which correspond to the pixels of ground measurements were computed and shown in Table 3.

Consequently, 4 datasets that belong to the different periods of 2015 and 2016 were formed as shown in Table 4.

Table 3. The obtained features for each pattern.

Feature name	Decomposition method
Double bounce	Freeman-Durden
Volume scattering	Freeman-Durden
Surface scattering	Freeman-Durden
Polarimetric entropy	H/A/α
Polarimetric anisotropy	H/A/α
σ_{hh}	Standard intensity and phase
σ_{hv}	Standard intensity and phase
σ_{vh}	Standard intensity and phase
σ_{vv}	Standard intensity and phase

Table 4. The details of formed datasets.

Datasets	Acquisition date	Dataset size
Dataset 1	27/02/2015	335*9
Dataset 2	08/04/2015	285*9
Dataset 3	10/06/2015	272*9
Dataset 4	03/03/2016	157*9

After that, different machine learning based regression techniques (SVR, ANFIS and GRNN) were employed for prediction of SWC on a yearly basis with aid of obtained features. Moreover, the leave-one-out cross validation was applied for validating system performance. The statistical error metrics: root mean square error (RMSE), mean absolute error (MAE) and correlation coefficient (R) were used as an index of the performance analysis. The results of different regression models were tabulated in Table 5.

Table 5. The performance of different regression models.

Model	Correlation (R)	RMSE	MAE
GRNN	0.86	3.53	2.54
SVM	0.81	4.06	3.00
ANFIS	0.76	4.63	3.20

The best performance was observed by GRNN model. Thus, we only considered the results of the GRNN based SWC prediction for the remaining applications in this work. For calculating the performance of the whole system, 2 approaches have been considered. In the first approach, training and testing sets were obtained from the datasets 1-2-3-4. Finally, the results of regression analysis between predicted and measured SWC values by utilizing GRNN and datasets 1-2-3-4 were indicated in Figure 4. The error of the whole system was computed as 8.36 vol. % RMSE, 5.97 vol. % MAE while the Pearson correlation coefficient (R) was 0.69.

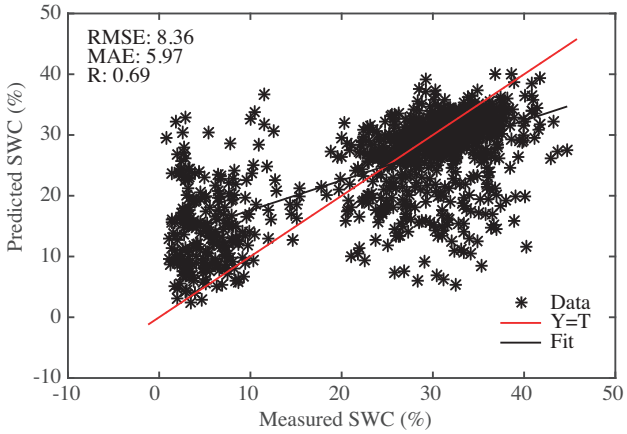

Figure 4. The regression between predicted and measured SWC values with all features and data sets 1-2-3-4.

In the second approach, the datasets were rearranged and the effect of no-vegetation period (June 2015) was neglected. Therefore, training and testing sets were acquired from the datasets 1-2-4 for prediction of SWC on a yearly basis. The obtained results for this case are shown in Figure 5.The error of entire system was computed as 3.89 vol. % RMSE, 2.98 vol. % MAE while the Pearson correlation coefficient (R) was 0.52.

3.2. SWC prediction with optimal features using ELM-FS method

In this scenario, the impact values of all features in 2 approaches as mentioned above were computed and ranked by ELM-FS method. The feature ranks were set on by the trained ELM's the output weights and multiplied with the reverse of the CV (coefficient of variation) of obtained parameters.

As seen in Table 6 (1st Approach), the most relevant features were selected with the aid of this rank and the overall performance of the prediction system was tabulated in Table 7.

Here, it can be seen that when the all features were employed, the obtained R was moderate high and RMSE value was low. On the other hand, when the selected features (especially, 8 features) were used, the obtained R and RMSE values were at the same level. Thus, we can say that the ELM-FS method does not only provide a reduction in the computational cost, but also represents less memory necessity and the appropriate

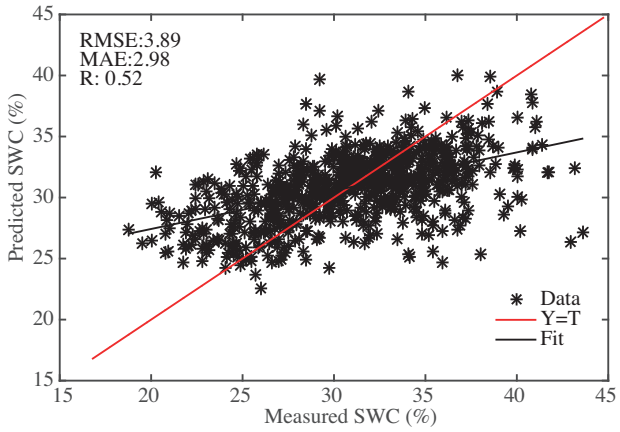

Figure 5. The regression between predicted and measured SWC by using all features and data sets 1-2-4 (without June 2015 data).

Table 6. Impact values and rank of all features for 1st Approach with ELM-FS method.

Rank of features	Feature name	Impact values
1	σ_{hv}	0.271
2	σ_{vh}	0.245
3	Volume scattering	0.238
4	Double scattering	0.133
5	σ_{hh}	0.046
6	Polarimetric entropy	0.017
7	σ_{vv}	0.013
8	Surface scattering	0.009
9	Polarimetric anisotropy	0.005

Table 7. Overall performance of the proposed model for Approach 1 using different feature set combinations.

Number of features	Number of selected features	Selected feature set	Feature reduction ratio (%)	RMSE	Correlation (R)
9	1	1	88.88	11.4078	0.1563
9	2	1, 2	77.77	11.4142	0.1516
9	3	1, 2, 3	66.66	11.2877	0.2127
9	4	1, 2, 3, 4	55.55	10.3676	0.4415
9	5	1, 2, 3,4,5	44.44	9.4222	0.5782
9	6	1, 2, 3,4,5,6	33.33	9.0545	0.6214
9	7	1, 2, 3,4,5,6,7	22.22	8.6153	0.6666
9	8	1, 2, 3,4,5,6,7,8	11.11	8.3636	0.6900

rank of the features. After that, the same procedure was employed to 2nd approach as well as the impact values of all features were computed and ranked by ELM-FS method as shown in Table 8.

By selecting the appropriate features according to the rank in Table 8, the performance of the whole system was tabulated in Table 9. It is obvious that the most dominant parameters in the 1st approach (σ_{vh}, σ_{hv} and volume scattering) are as same as in the 2nd approach.

As seen in Table 9, we observed that when the all features were used, the obtained R was moderate and RMSE value was so low. However, when the selected features were utilized, the computed R and RMSE values exhibited the higher performance with 33.33 % feature reduction ratio (only 6 features).

Taking everything into account, the main contribution of this study is to obtain feature vectors with a new approach and to predict SWC on a yearly basis over the bare and vegetation-covered fields by employing different machine learning techniques and ELM based feature selection method.

Looking at the literature studies, some studies for the prediction of soil surface parameters using satellite data and machine learning techniques are presented in Table 10. The overall performance of the proposed system is in the acceptable range compared to the other approaches as seen in Table 10.

Table 8. Impact values and ranking of all features for 2nd Approach with ELM-FS method.

Rank of features	Feature name	Impact values
1	σ_{vh}	0.255
2	σ_{hv}	0.238
3	Volume scattering	0.234
4	Double scattering	0.156
5	σ_{hh}	0.063
6	Surface scattering	0.027
7	σ_{vv}	0.014
8	Polarimetric entropy	0.012
9	Polarimetric anisotropy	0.008

Table 9. Overall performance of the proposed model for Approach 2 using different feature set combinations.

Number of features	Number of selected features	Selected feature set	Feature reduction ratio (%)	RMSE	Correlation (R)
9	1	1	88.88	4.4134	0.2020
9	2	1,2	77.77	4.4058	0.2101
9	3	1,2,3	66.66	4.4010	0.2161
9	4	1,2,3,4	55.55	4.0517	0.4376
9	5	1,2,3,4,5	44.44	4.0286	0.4522
9	6	1,2,3,4,5,6	33.33	3.8731	0.5145
9	7	1,2,3,4,5,6,7	22.22	3.8969	0.5110
9	8	1,2,3,4,5,6,7,8	11.11	3.8894	0.5241

4. Conclusion

In this study, different machine learning based inversion techniques with a feature selection method was recommended for prediction of the SWC on a yearly basis over the croplands with the help of fully polarimetric

Table 10. The comparison of some literature studies which are related with the prediction of soil surface parameters by using satellite data and machine learning techniques.

Satellite data	RMSE (%)	Approach	Reference
Radarsat-2	3.80	Polarimetric decomposition GRNN SVR ANFIS ELM-FS	Proposed approach
Advanced Microwave scanning Radiometer-2	3.83	Deep learning	[47]
Radarsat-2 Cosmo-SkyMed	2.0- 4.0	SVR ANN	[48]
Sentinel-1	3.0	Random forest	[49]
Radarsat-2	7.12	Adaptive two component	[50]
Radarsat-1	4.0–6.5	ANN Fuzzy logic	[51]

SAR features. In the feature extraction stage, the feature vector for each pattern was obtained by employing the standard intensity/phase and polarimetric decomposition models. Then, totally 9 features, which correspond to the pixels of each ground measurement point were constituted. By merging the feature vectors, 4 datasets, which belong to the different periods of 2015 and 2016, were created. After that, ELM-FS based a new feature selection algorithm was implemented for determining the optimal features of the recommended system. Two scenarios of SM prediction were considered for this system. In the first scenario, all features were utilized as inputs of machine learning based prediction techniques (SVR, ANFIS and GRNN) and in the second scenario, the most suitable features were determined with the aid of the ELM-FS method. At the end, a feature set with 6 parameters was determined as most optimal feature set over the SWC prediction and a slightly better performance was observed thanks to this feature set compared to the first scenario results. In addition, low operational cost and memory demand have been achieved thanks to the ELM-FS.

In the future, it is planned to use different spectral band features and local measurement data for improving the accuracy of the proposed system. Furthermore, the various feature extraction methods and machine learning techniques will be analyzed for surface parameter predictions. It is thought that improving this system will assist that the water resources will be utilized more effectively and the amount of those resources will be automatically controlled for irrigation.

Acknowledgment

The authors would like to thank European Space Agency (ESA) for Sentinel-1 software. This study was supported by The Scientific and Technological Research Council of Turkey (TÜBİTAK) 1001 (No. 114E543) research project and Dicle University Scientific Research Projects Unit (DUBAP) and TARBIL (Agricultural Monitoring and Information System) project.

References

[1] Hajnsek I, Jagdhuber T, Schon H, Papathanassiou KP. Potential of estimating soil moisture under vegetation cover by means of PolSAR. IEEE Transactions on Geoscience and Remote Sensing 2009; 47: 442-454. doi: 10.1109/TGRS.2008.2009642

[2] Gorrab A, Zribi M, Baghdadi N, Mougenot B, Chabaane Z. Potential of X-band TerraSAR-X and COSMO-SkyMed SAR data for the assessment of physical soil parameters. Remote Sensing 2015; 7 (1): 747-766. doi: 10.3390/rs70100747

[3] Thoma DP, Moran MS, Bryant R, Rahman M, Holifield-Collins CD et al. Comparison of four models to determine surface soil moisture from C-band radar imagery in a sparsely vegetated semiarid landscape. Water Resources Research 2006; 42 (1). doi: 10.1029/2004WR003905

[4] Oliver C, Quegan S. Understanding Synthetic Aperture Radar Images. Stevenage, UK: SciTech Publishing, 2004.

[5] He B, Xing M, Bai X. A synergistic methodology for soil moisture estimation in an alpine prairie using radar and optical satellite data. Remote Sensing 2014; 6 (11): 10966-10985. doi: 10.3390/rs61110966

[6] Jagdhuber T, Hajnsek I, Papathanassiou KP. An iterative generalized hybrid decomposition for soil moisture retrieval under vegetation cover using fully polarimetric SAR. IEEE Journal of Selected Topics in Applied Earth Observations and Remote Sensing 2014; 8 (8): 3911-3922. doi: 10.1109/JSTARS.2014.2371468

[7] Baghdadi N, Holah N, Zribi M. Soil moisture estimation using multi-incidence and multi-polarization ASAR data. International Journal of Remote Sensing 2006; 27: 1907-1920. doi: 10.1080/01431160500239032

[8] Xiaodong H, Jinfei W, Jiali S. Adaptive two-component model-based decomposition on soil moisture estimation for c-band Radarsat-2 imagery over wheat fields at early growing stages. IEEE Geoscience and Remote Sensing Letters 2016; 13: 414-418.

[9] Arii M, Van ZJ, Jakob J, Kim Y. A general characterization for polarimetric scattering from vegetation canopies. IEEE Transactions on Geoscience and Remote Sensing 2010; 48 (9): 3349-3357. doi: 10.1109/TGRS.2010.2046331

[10] Bai X, He B, Li X. Optimum surface roughness to parameterize advanced integral equation model for soil moisture retrieval in prairie area using Radarsat-2 data. IEEE Transactions on Geoscience and Remote Sensing 2016; 5: 42437-2449. doi: 10.1109/TGRS.2015.2501372

[11] Oh Y, Sarabandi K, Ulaby FT. An empirical model and an inversion technique for radar scattering from bare soil surfaces. IEEE Transactions on Geoscience and Remote Sensing 1992; 30: 370-381.

[12] Fung AK, Chen KS. An update on the IEM surface backscattering model. IEEE Geoscience and Remote Sensing Letters 2004; 1: 75-77. doi:10.1109/LGRS.2004.826564

[13] Notarnicola C, Angiulli M, Posa F. Soil moisture retrieval from remotely sensed data: Neural network approach versus Bayesian method. IEEE Transactions on Geoscience and Remote Sensing 2008; 46: 547-557. doi: 10.1109/TGRS.2007.909951

[14] Zhang X, Chen B, Fan H, Huang J, Zhao H. The potential use of multi-band SAR data for soil moisture retrieval over bare agricultural areas: Hebei, China. Remote Sensing 2016; 8: 7. doi: 10.3390/rs8010007

[15] Pasolli L, Notarnicola C, Bruzzone L. Estimating soil moisture with the support vector regression technique. IEEE Geoscience and Remote Sensing Letters 2011; 8: 1080-1084. doi: 10.1109/LGRS.2011.2156759

[16] Ahmad S, Kalra A, Stephen H. Estimating soil moisture using remote sensing data: A machine learning approach. Advances in Water Resources 2010; 33: 69-80. doi:10.1016/j.advwatres.2009.10.008

[17] Pasolli L, Notarnicola C, Bruzzone L, Bertoldi G, Chiesa SD et al. Polarimetric RADARSAT-2 imagery for soil moisture retrieval in alpine areas. Canadian Journal of Remote Sensing 2011; 37: 535-547.doi:10.5589/m11-065

[18] Said S, Kothyari UC,Arora M K. ANN-based soil moisture retrieval over bare and vegetated areas using ERS-2 SAR data. Journal of Hydrologic Engineering 2008; 13 (6): 461-475. doi: 10.1061/(ASCE)1084-0699

[19] Zhang X, Chen B, Fan H, Huang J, Zhao H. The potential use of multi-band SAR data for soil moisture retrieval over bare agricultural areas: Hebei, China. Remote Sensing 2016; 8 (1): 7. doi: 10.3390/rs8010007

[20] Weimann A. Inverting a microwave backscattering model by the use of a neural network for the estimation of soil moisture. In: Proc IGARSS; Seattle-USA; 1998. pp. 1837-1839.

[21] Paloscia S, Pampaloni P, Pettinato S, Santi E. A comparison of algorithms for retrieving soil moisture from ENVISAT/ASAR images. IEEE Transactions on Geoscience and Remote Sensing 2008; 46 (10): 3274-3284. doi: 0.1109/TGRS.2008.920370

[22] Srivastava PK, Han D, Ramirez MR, Islam T. Machine learning techniques for downscaling SMOS satellite soil moisture using MODIS land surface temperature for hydrological application. Water Resources Management 2013; 27 (8): 3127-3144. doi: 10.1007/s11269-013-0337-9

[23] Xie XM, Xu JW, Zhao JF, Liu S, Wang P. Soil moisture inversion using AMSR-E remote sensing data: An artificial neural network approach. Applied Mechanics and Materials 2014; 501: 2073-2076. doi: 10.4028/AMM.501-504.2073

[24] Yadav B, Ch S, Mathur S, Adamowski J. Assessing the suitability of extreme learning machines (ELM) for groundwater level prediction. Journal of Water and Land Development 2017; 32 (1): 103-112.

[25] Liu Y, Mei L, Ooe SK. Prediction of soil moisture based on extreme learning machine for an apple orchard. In: Conference on IEEE Computational Interdisciplinary Science; Shenzhen-China; 2014. pp. 400-404.

[26] Prasad R, Deo RC, Li Y, Maraseni T. Soil moisture forecasting by a hybrid machine learning technique: ELM integrated with ensemble empirical mode decomposition. Geoderma 2018; 330: 136-161. doi: 10.1016/j.geoderma.2018.05.035

[27] Marcano-Cedeno A, Quintanilla-Dom J, Cortina-Januchs MG, Andina D. Feature selection using sequential forward selection and classifcation applying artifcial metaplasticity neural network. In: Proceedings of the 36th Annual Conference of the IEEE Industrial Electronics Society; Glendale-USA; 2010. pp. 2845-2850.

[28] Somol P, Pudil P, Kittler J. Fast branch & bound algorithms for optimal feature selection. IEEE Transactions on Pattern Analysis and Machine Intelligence 2004; 26 (7): 900-912. doi: 10.1109/TPAMI.2004.28

[29] Pang Z, Zhu D, Chen D, Li L, Shao Y. A computer-aided diagnosis system for dynamic contrast-enhanced MR images based on level set segmentation and ReliefF feature selection. Computational and Mathematical Methods in Medicine 2015. doi: 10.1155/2015/450531

[30] Chandrashekar G, Sahin F. A survey on feature selection methods.Computers & Electrical Engineering 2014; 40 (1): 16-28. doi: 10.1016/j.compeleceng.2013.11.024

[31] Xue B, Zhang M, Browne WN, Yao X. A survey on evolutionary computation approaches to feature selection. IEEE Transactions on Evolutionary Computation 2016; 20 (4): 606-626. doi: 10.1109/TEVC.2015.2504420

[32] Ertuğrul ÖF, Tağluk ME. A fast feature selection approach based on extreme learning machine and coefficient of variation. Turkish Journal of Electrical Engineering and Computer Sciences 2017; 25 (4): 3409-3420. doi: 10.3906/elk-1606-122

[33] Veci L. Sentinel-1 Toolbox: SAR Basics Tutorial. Paris, FR: ARRAY Systems Computing, Incorporation and European Space Agency, 2015.

[34] Özerdem MS, Acar E, Ekinci R. Soil moisture estimation over vegetated agricultural areas: Tigris Basin, Turkey from Radarsat-2 data by polarimetric decomposition models and a generalized regression neural network. Remote Sensing 2017; 9: 395. doi: 10.3390/rs9040395

[35] Sakshaug SEH. Evaluation of polarimetric SAR decomposition methods for tropical forest analysis. Master Thesis, University of Tromsø, Tromsø, Norway, 2013.

[36] Freeman A, Durden SL. A three-component scattering model for polarimetric SAR data. IEEE Transactions on Geoscience and Remote Sensing 1998; 36 (3): 963-973. doi: 10.1109/36.673687

[37] Lee JS, Eric P. Polarimetric Radar Imaging: From Basics to Applications. USA: CRC Press, 2009.

[38] Cloude SR, Pottier E. An entropy based classification scheme for land applications of polarimetric SAR. IEEE Transactions on Geoscience and Remote Sensing 1997; 35 (1): 68-78. doi: 10.1109/36.551935

[39] Specht DF. A general regression neural network. IEEE Transactions on Neural Networks 1991; 2 (6): 568-576.

[40] Li W, Yang X, Li H, Su L. Hybrid forecasting approach based on GRNN neural network and SVR machine for electricity demand forecasting. Energies 2017; 10 (1): 44. doi: 10.3390/en10010044

[41] Thipparat T. Application of adaptive neuro fuzzy inference system in supply chain management evaluation. In: Dadios EP (editor). Fuzzy Logic—Algorithms, Techniques and Implementations. London, UK: IntechOpen, 2012, pp. 115-126.

[42] Huang GB, Zhu QY, Siew CK. Extreme learning machine: theory and applications. Neurocomputing 2006; 70: 489-501. doi: 10.1016/j.neucom.2005.12.126

[43] Huang GB, Zhu QY, Siew CK. Extreme learning machine: a new learning scheme of feedforward neural networks. In: IEEE 2004 Neural Networks Conference; 2004; Budapest- Hungary and New York-USA; 2004. pp. 985-990.

[44] Huang GB, Wang DH, Lan Y. Extreme learning machines: a survey. International Journal of Machine Learning and Cybernetics 2011; 2: 107-122. doi:10.1007/s13042-011-0019-y

[45] Huang GB. An insight into extreme learning machines: random neurons, random features and kernels. Cognitive Computation 2014; 6: 376-390. doi: 10.1007/s12559-014-9255-2

[46] Wang R, Kwong S, Wang X. A study on random weights between input and hidden layers in extreme learning machine. Soft Computing 2012; 16: 1465-1475. doi: 10.1007/s00500-012-0829-1

[47] Chang SL, Eunha S, Jun DP, Jae-Dong J. Estimation of soil moisture using deep learning based on satellite data: a case study of South Korea. GIScience & Remote Sensing, 2019; 56 (1): 43-67. doi: 10.1080/15481603.2018.1489943

[48] Santi E, Pettinato S, Paloscia S, Dabboor M, Notarnicola C et al. Estimating soil moisture from C and X Band Sar using machine learning algorithms and compact polarimetry. In: IGARSS 2018-2018 IEEE International Geoscience and Remote Sensing Symposium; New York, USA; 2018. pp. 1426-1429.

[49] Hajdu I, Yule I, Dehghan-Shear MH. Modelling of near-surface soil moisture using machine learning and multi-temporal Sentinel 1 images in New Zealand. In: IGARSS 2018-2018 IEEE International Geoscience and Remote Sensing Symposium; Valencia-Spain; 2018. pp. 1422-1425.

[50] Huang X, Wang J, Shang J. An adaptive two-component model-based decomposition on soil moisture estimation for C-band Radarsat-2 imagery over wheat fields at early growing stages. IEEE Geoscience and Remote Sensing Letters 2016; 13 (3): 414-418. doi: 10.1109/LGRS.2016.2517082

[51] Lakhankar T, Ghedira H, Temimi M, Sengupta M, Khanbilvardi R et al. Non-parametric methods for soil moisture retrieval from satellite remote sensing data. Remote Sensing 2009; 1 (1): 3-21. doi: 10.3390/rs1010003